AMERICAN SOCIETY FOR MICROBIOLOGY | Applied and Environmental Microbiology®

GENETICS AND MOLECULAR BIOLOGY

The Lectin Chaperone Calnexin Is Involved in the Endoplasmic Reticulum Stress Response by Regulating Ca^{2+} Homeostasis in *Aspergillus nidulans*

Shenghua Zhang,[a] Hailin Zheng,[a]* Qiuyi Chen,[a] Yuan Chen,[a] Sha Wang,[a,b] Ling Lu,[a] Shizhu Zhang[a]

Jiangsu Key Laboratory for Microbes and Functional Genomics, Jiangsu Engineering and Technology Research Center for Microbiology, College of Life Sciences, Nanjing Normal University, Nanjing, China[a]; Program in Molecular and Translational Medicine (PMTM), School of Medicine, Huzhou University, Huzhou, China[b]

ABSTRACT The Ca^{2+}-mediated signaling pathway is crucial for environmental adaptation in fungi. Here we show that calnexin, a molecular chaperone located in the endoplasmic reticulum (ER), plays an important role in regulating the cytosolic free calcium concentration ($[Ca^{2+}]_c$) in *Aspergillus nidulans*. Inactivation of calnexin (ClxA) in *A. nidulans* caused severe defects in hyphal growth and conidiation under ER stress caused by the ER stress-inducing agent dithiothreitol (DTT) or high temperature. Importantly, defects in the Δ*clxA* mutant were restored by the addition of extracellular calcium. Furthermore, the CchA/MidA complex (the high-affinity Ca^{2+} channels), calcineurin (calcium/calmodulin-dependent protein phosphatase), and PmrA (secretory pathway Ca^{2+} ATPase) were required for extracellular calcium-based restoration of the DTT/thermal stress sensitivity in the Δ*clxA* mutant. Interestingly, the Δ*clxA* mutant exhibited markedly reduced conidium formation and hyphal growth defects under the low-calcium condition, which is similar to defects caused by mutations in MidA/CchA. Moreover, the phenotypic defects were further exacerbated in the Δ*clxA* Δ*midA* Δ*cchA* mutant, which suggested that ClxA and MidA/CchA are both required under the calcium-limiting condition. Using the calcium-sensitive photoprotein aequorin to monitor $[Ca^{2+}]_c$ in living cells, we found that ClxA and MidA/CchA complex synergistically coordinate transient increase in $[Ca^{2+}]_c$ in response to extracellular calcium. Moreover, ClxA, in particular its luminal domain, plays a role in mediating the transient $[Ca^{2+}]_c$ in response to DTT-induced ER stress in the absence of extracellular calcium, indicating ClxA may mediate calcium release from internal calcium stores. Our findings provide new insights into the role of calnexin in the regulation of calcium-mediated response in fungal ER stress adaptation.

IMPORTANCE Calnexin is a well-known molecular chaperone conserved from yeast to humans. Although it contains calcium binding domains, little is known about the role of calnexin in Ca^{2+} regulation. In this study, we demonstrate that calnexin (ClxA) in the filamentous fungus *Aspergillus nidulans*, similar to the high-affinity calcium uptake system (HACS), is required for normal growth and conidiation under the calcium-limiting condition. The ClxA dysfunction decreases the transient cytosolic free calcium concentration ($[Ca^{2+}]_c$) induced by a high extracellular calcium or DTT-induced ER stress. Our findings provide the direct evidence that calnexin plays important roles in regulating Ca^{2+} homeostasis in addition to its role as a molecular chaperone in fungi. These results provide new insights into the roles of calnexin and expand knowledge of fungal stress adaptation.

KEYWORDS *Aspergillus nidulans*, ER stress, calcium signaling

Received 22 March 2017 **Accepted** 18 May 2017

Accepted manuscript posted online 26 May 2017

Citation Zhang S, Zheng H, Chen Q, Chen Y, Wang S, Lu L, Zhang S. 2017. The lectin chaperone calnexin is involved in the endoplasmic reticulum stress response by regulating Ca^{2+} homeostasis in *Aspergillus nidulans*. Appl Environ Microbiol 83:e00673-17. https://doi.org/10.1128/AEM.00673-17.

Editor Dan Cullen, USDA Forest Products Laboratory

Address correspondence to Shizhu Zhang, szzhang@njnu.edu.cn.

* Present address: Hailin Zheng, Department of Medical Mycology, Institute of Dermatology, Chinese Academy of Medical Science and Peking Union Medical College, Nanjing, China.

Shenghua Zhang and Hailin Zheng contributed equally to this article.

The Ca^{2+}-mediated signaling pathway plays a crucial role in fungal survival under various stresses (1, 2). Upon stimulation, the plasma membrane Ca^{2+} influx system is activated, resulting in rapid Ca^{2+}influx, which is directly sensed by the central Ca^{2+} sensor calmodulin and subsequently retransmitted to cellular targets (3, 4). The best-studied Ca^{2+}-responsive signaling pathway in fungi involves the calcineurin and calcineurin-dependent dephosphorylation of Crz1, a zinc finger transcription factor (5–7). Subsequently, an increased cytosolic free calcium concentration ($[Ca^{2+}]_c$) returns to its normally low resting level within the cytosol due to various calcium pumps and calcium antiporters, as well as cytoplasmic calcium buffering (8, 9). Two different calcium carrier systems have been identified in most fungal species: the high-affinity Ca^{2+} influx system (HACS) and the low-affinity calcium influx system (LACS) (10–13). The main components of the HACS are an α subunit of the mammalian voltage-gated Ca^{2+}-channel homolog Cch1 and a stretch-activated β subunit called Mid1 (14–16). Loss of the HACS results in an inability to grow under low-calcium conditions. Fig1 is the only characterized member of the LACS in fungi, and in *Saccharomyces cerevisiae* Fig1 facilitates Ca^{2+} influx and cell fusion during mating (12).

Besides Ca^{2+} taken up from the extracellular environment, the Ca^{2+} released from internal calcium pools such as the endoplasmic reticulum (ER) and vacuoles is also valuable to increase intracellular Ca^{2+} concentrations (17, 18). The ER is a specialized organelle responsible for multiple functions, including the synthesis and processing of secreted proteins and lipid metabolism. High Ca^{2+} concentrations are required for the activities of numerous enzymes in the ER. In *S. cerevisiae*, the concentration of Ca^{2+} in the ER is approximately 100-fold greater than that in the cytoplasm and even higher in mammalian cells (18–20). In mammalian cells, calcium transport to the endoplasmic/sarcoplasmic reticulum is mediated by sarco-endoplasmic reticulum Ca^{2+} ATPases (SERCA) (21, 22). Yeast cells lack homologs of the SERCA pumps but express Pmr1p, a homolog of mammalian secretory pathway Ca^{2+} ATPases (SPCAs). Pmr1p is the functional equivalent of mammalian SERCA, and the mutant lacking *pmr1p* accumulated only half as much Ca^{2+} in the ER (19, 23). Different stimuli can disrupt ER function, including calcium depletion from the ER lumen (24, 25). Rapid Ca^{2+} release lowers the Ca^{2+} concentration in the ER and elevates free Ca^{2+} levels in the cytosol, which can then activate various signal transduction pathways (26). Evidence indicates that one response to ER stress is the stimulation of Ca^{2+} influx across the plasma membrane through HACS, which serves to replenish the Ca^{2+}-depleted ER stores in both animal and yeast cells (25, 26).

Besides calcium pumps, Ca^{2+}-binding proteins in the ER lumen are thought to play important roles in maintaining Ca^{2+} concentrations in the ER. Calnexin is a type I transmembrane protein, and calnexin and its lumenal soluble homolog calreticulin are known to be the two major calcium-binding proteins of the ER in mammalian cells (27, 28). However, only calnexin has been identified in most fungal species (29). As a key ER chaperone, calnexin promotes protein folding and prevents aggregation by binding to nascent glycoproteins as they enter the ER (30, 31). To date, the function of calnexin as a chaperone is well documented (32, 33). In addition to its role as a molecular chaperone, calnexin is also capable of binding Ca^{2+} and has been proposed to be involved in the retention of soluble ER proteins in a Ca^{2+}-dependent manner (27). Calnexin possesses four characteristic KPEDWDE motifs, which have been suggested to represent the high-affinity calcium binding domain of calnexin and calreticulin (34, 35). One exception is calnexin from *S. cerevisiae*, which contains only a single copy of the KPEDWD repeat domain. Consistent with their characteristic structure, all calnexins and calreticulins tested thus far bind calcium, except for *S. cerevisiae* Cne1P (34, 36, 37). Although it contains a calcium binding domain, little is known about the role of calnexin in Ca^{2+} regulation. In *Schizosaccharomyces pombe*, the expression of Cnx1 can be induced by the calcium ionophore A23187, indicating that Cnx1 plays a role in Ca^{2+} regulation or sequestration (34). However, direct evidence for this effect is still lacking.

Aspergillus species are among the most abundant fungi worldwide. Among them,

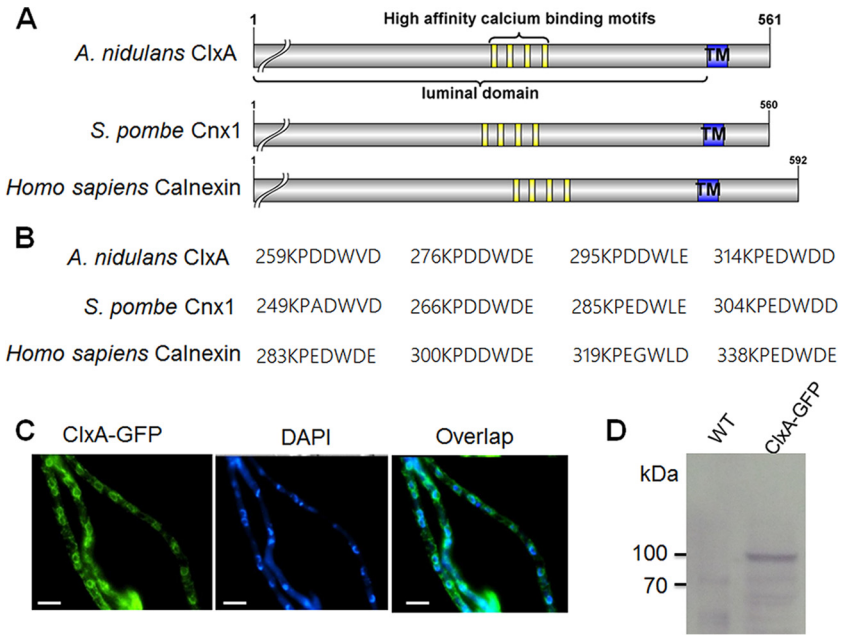

FIG 1 Bioinformatic identification and subcellular location of ClxA. (A) Schematic representation of the conserved motifs of calnexin homologs in *A. nidulans*, *S. pombe*, and *H. sapiens*. The cutline indicates the position of the predicted cleavable signal peptide. TM, transmembrane domain. (B) Comparision of predicted high-affinity calcium binding motifs. The numbers denote the place on the original sequence of the first residue in the motif. (C) ClxA localizes in the ER as shown by using GFP-tagged fusion proteins. DAPI (4[prime],6-diamidino-2-phenylindole) was used to visualize nuclei. (D) Western blot analysis using an anti-GFP antibody detected a fusion protein of ClxA-GFP with a size of approximately 100 kDa.

Aspergillus nidulans has been used as a model organism to study many biological processes and fungal stress adaptation. In this study, we found that an *A. nidulans clxA* null mutant was sensitive to ER stress-inducing agent dithiothreitol (DTT) and thermal stress and that this phenotype could be rescued by the addition of extracellular calcium. Moreover, using codon-optimized aequorin as a calcium reporter in living cells, we found that *clxA* dysfunction significantly decreased the amplitude of the transient $[Ca^{2+}]_c$ induced by extracellular calcium and dithiothreitol (DTT) stimulation. Furthermore, we showed that ClxA—in particular its luminal domain—plays an important role in regulating Ca^{2+} homeostasis in response to ER stress.

RESULTS

Identification of a calnexin homolog in *A. nidulans*. Using NCBI BLASTp (http://www.ncbi.nlm.nih.gov/BLAST/), we identified a putative *A. nidulans* ortholog of the *Homo sapiens* and *S. pombe* calnexin/calreticulin, referred to as ClxA (AN3592.4; GenBank accession no. CBF75819.1). ClxA is a 561-amino-acid protein that showed 46.4% and 38.7% identities to *S. pombe* and *Homo sapiens* calnexin, respectively. Bioinformatic analysis revealed ClxA shares a similar overall arrangement to *H. sapiens* and *S. pombe* calnexin, with a predicted N-terminal cleavable signal sequence, a transmembrane domain proximal to a cytoplasmic domain, and importantly, four repeats of the KPE DWDE motif (Fig. 1A and B). The KPEDWDE motif repeats are conserved in almost all calnexins and have been suggested to be high-affinity calcium binding sites (34, 35). Microscopic examination of a ClxA-green fluorescent protein (GFP) fusion protein showed that ClxA was predominantly localized to the endoplasmic reticulum (ER), with a network of strands around the peripheral nuclear envelope (Fig. 1C). Furthermore, Western blotting was performed to verify the expression of the fusion protein. After accounting for GFP as a 27-kDa protein, the relative molecular mass of ClxA was approximately 73 kDa, which is clearly higher than the predicted molecular mass of 62 kDa (Fig. 1D). This anomalous migration on SDS-PAGE was

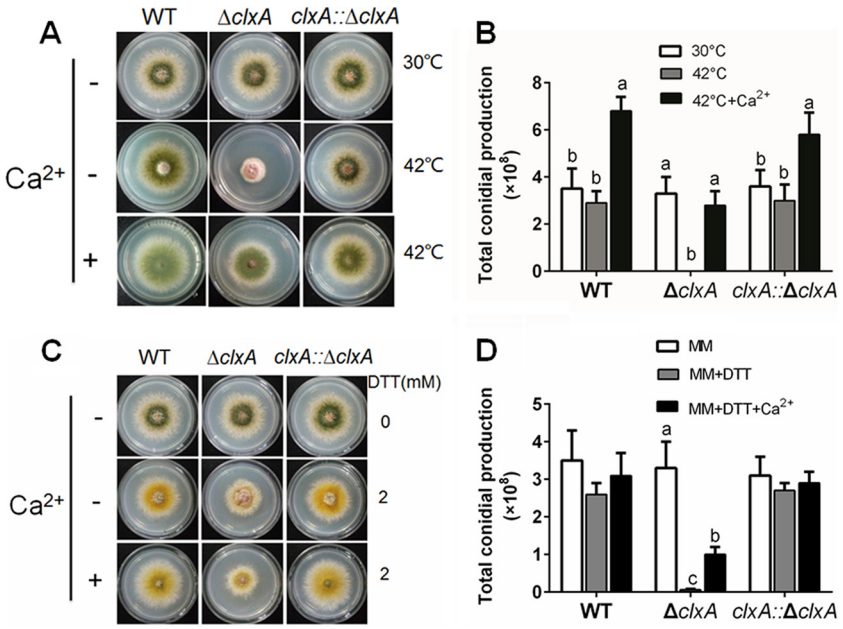

FIG 2 The sensitivity to thermal/DTT stress in the Δ*clxA* mutant can be restored by extracellular calcium. (A) Colony morphology comparison for the indicated strains grown on solid MM in the presence or absence of 200 mM $CaCl_2$ at 30 or 42°C for 2.5 days. (B) Quantitative total conidial production for the strains shown in panel A. (C) Colony morphology comparison for the indicated strains grown on solid MM in the presence or absence of 200 mM $CaCl_2$ and/or 2 mM DTT at 30°C for 2.5 days. (D) Quantitative total conidial production for the strains shown in panel C. Error bars represent standard deviations from three replicates. Different lowercase letters on the bars of each group represent significant differences among strains (Tukey's multiple-comparison test, $P < 0.05$).

also observed for *S. pombe* calnexin (Cnx1), which has a predicted molecular mass of 63 kDa compared to the apparent molecular mass of 91 kDa. Posttranslational modifications such as N-glycosylation are likely to be responsible for the discrepancy (27, 34).

Sensitivity to thermal/DTT stress in the Δ*clxA* mutant can be restored by extracellular calcium. To explore the function of the *clxA* gene, a *clxA* null mutant (Δ*clxA*) was generated by homologous recombination in which the *clxA* open reading frame (ORF) was replaced with the *pyr4* selectable marker. Diagnostic PCR confirmed that the Δ*clxA* strain had the correct insertion of the *pyr4* disruption cassette, and no original *clxA* ORF was detected (see Fig. S1 in the supplemental material). As shown in Fig. 2A and B, there were no detectable differences between the Δ*clxA* mutant and the parental wild-type (WT) strain when grown at 30°C on minimal medium (MM). In comparison, the hyphal radial growth of the Δ*clxA* mutant at 42°C showed a 29% ± 2.1% reduction compared to the parental wild-type strain. Moreover, the loss of *clxA* dramatically increased hyphal branching frequencies compared to that in the wild type under thermal stress (see Fig. S2 in the supplemental material). Conidiation in the Δ*clxA* mutant was almost abolished at 42°C. As expected, the expression of *brlA*, a center regulator of conidiation was dramatically reduced in the Δ*clxA* mutant under heat stress (see Fig. S3 in the supplemental material). Next, we compared the growth of the Δ*clxA* mutant and the parental wild-type strain in the presence of dithiothreitol (DTT), a reducing agent that disrupts disulfide bonds. Consistent with the results obtained from the thermal stress test (culture at 42°C), hyphal radial growth and total conidium production in the Δ*clxA* mutant on MM plus 2 mM DTT decreased to 74% ± 3.1% and 2% ± 0.6%, respectively, compared to that of cultures grown on MM alone (Fig. 2C and D). In contrast, there were minimal effects on the parental wild-type strain under the same test conditions, except for the production of yellow conidia under DTT stress. In addition, ectopically expressed *clxA* was able to completely rescue these defects in the

Δ*clxA* mutant strain, showing that these phenotypes were specifically due to the loss of *clxA*.

Importantly, we found that sensitivity to thermal stress in the Δ*clxA* mutant could be dramatically restored by the addition of extracellular calcium. Moreover, restoration of the defective phenotypes showed a dose-dependent response to calcium addition. Interestingly, the addition of calcium could boost the growth and conidiation of the parental wild type to some extent under thermal stress (see Fig. S4 in the supplemental material). As mentioned above, the conidiation of the Δ*clxA* mutant was almost abolished at 42°C. However, when the Δ*clxA* mutant was grown in the presence of 200 mM $CaCl_2$ at 42°C, the total conidium production reached 45% ± 6.4% of that of the parental wild-type strain (Fig. 2A and B). Accordingly, total conidium production in the Δ*clxA* mutant increased from 3% ± 1.2% on MM with 2 mM DTT to 32% ± 6.2% on MM with 2 mM DTT plus 200 mM $CaCl_2$, compared to the reference strain (Fig. 2C and D). Collectively, the above results showed that extracellular calcium could restore the growth and conidiation defects seen in the Δ*clxA* mutant under ER stress caused by high temperature or DTT.

MidA and CchA are required for the extracellular calcium-based restoration of DTT/thermal stress sensitivity in the Δ*clxA* mutant. The HACS components MidA and CchA are required for Ca^{2+} influx from the extracellular environment (14). To investigate if MidA and CchA are required for the extracellular calcium-based restoration of thermal/DTT sensitivity in the Δ*clxA* mutant, a Δ*clxA* Δ*midA* Δ*cchA* mutant was generated by genetic crossing of Δ*clxA* and Δ*midA* Δ*cchA* mutants, as described in Materials and Methods. Consistent with our previous report (14), the Δ*midA* Δ*cchA* mutant showed a smaller colony size with decreased conidium production compared to that of the parental wild type when grown on MM. Thermal stress or the addition of 2 mM DTT to MM further aggravated the hyphal growth and conidiation defects. Hyphal radial growth and the total conidium production in the Δ*midA* Δ*cchA* mutant at 42°C were decreased by 12% ± 0.4% and 66% ± 6.2%, respectively, compared with those at 30°C (Fig. 3A and B). Furthermore, the hyphal radial growth and the total conidium production in the Δ*midA* Δ*cchA* mutant showed 12% ± 0.5% and 61% ± 19% reductions, respectively, on MM plus 2 mM DTT compared with colonies grown on MM alone (Fig. 3C and D). These results suggested that *midA* and *cchA* were involved in fungal thermal and DTT tolerance. As expected, exogenous Ca^{2+} substantially restored the defects seen in the Δ*midA* Δ*cchA* mutant under either thermal or DTT stress.

In comparison, the Δ*clxA* Δ*midA* Δ*cchA* mutant showed more severe hyphal radial growth and conidiation defects than the Δ*midA* Δ*cchA* or Δ*clxA* mutants on MM at 30°C. Conidiation in the Δ*clxA* Δ*midA* Δ*cchA* mutant was almost completely abolished even at 30°C (Fig. 3A and B). Moreover, thermal stress or the addition of 2 mM DTT on MM further aggravated the defects seen in the Δ*clxA* Δ*midA* Δ*cchA* mutant. However, contrary to the Δ*clxA* and Δ*midA* Δ*cchA* mutants, in which extracellular calcium restored the hyphal radial growth and conidiation defects, the addition of calcium could not restore the defects in the Δ*clxA* Δ*midA* Δ*cchA* mutant under DTT stress, but could partially restore the defects under thermal stress. The total conidium production in the Δ*clxA* Δ*midA* Δ*cchA* mutant was 17% ± 3.3% compared to that in the Δ*clxA* mutant when supplemented with 200 mM $CaCl_2$ at 42°C. Taken together, the above results suggested that ClxA and MidA/CchA coordinate the fungal ER stress response. The MidA/CchA channels are required for extracellular calcium-based restoration of the hyphal radial growth and conidiation defects seen in the Δ*clxA* mutant under DTT or thermal stress.

DTT/thermal stress sensitivity in the Δ*clxA* mutant can be rescued by extracellular Ca^{2+} in a calcineurin-dependent manner. Extracellular $CaCl_2$ results in calcium uptake and a transient increase in $[Ca^{2+}]_c$, which leads to calcineurin activation and subsequent Crz1 dephosphorylation (1, 7). To investigate the relationship between calcineurin and *clxA*, *cnaA* (encoding the α subunit of calcineurin) was deleted in the Δ*clxA* mutant background. Consistent with our previous report, the Δ*cnaA* strain displayed a compact colony morphology with severe defects in hyphal radial growth

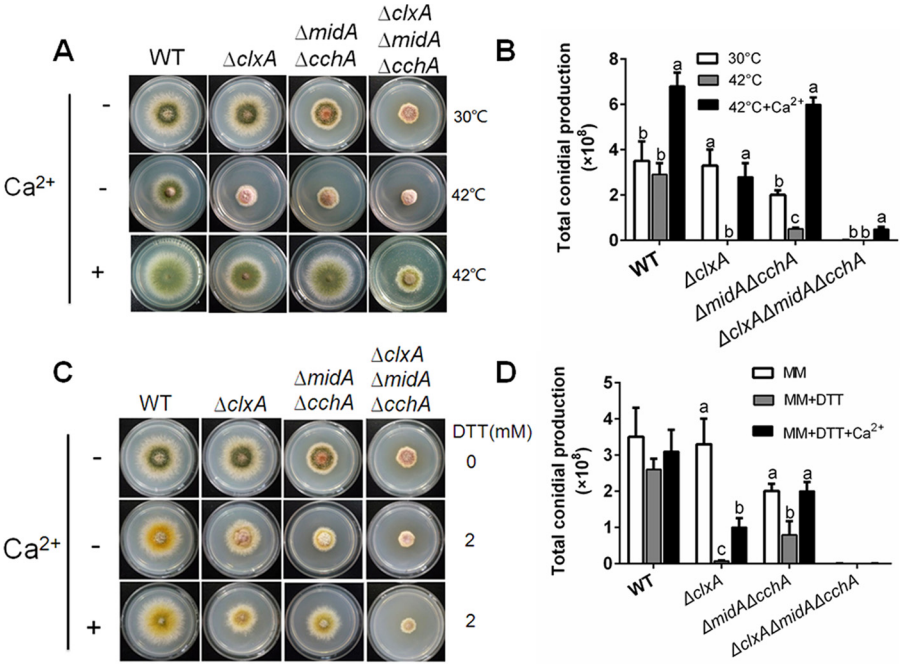

FIG 3 MidA and CchA are required for the extracellular calcium-based restoration of the DTT/thermal stress sensitivity in the Δ*clxA* mutant. (A) Colony morphology comparison for the indicated strains grown on solid MM in the presence or absence of 200 mM $CaCl_2$ at 30 or 42°C for 2.5 days. (B) Quantitative total conidial production for the strains shown in panel A. (C) Colony morphology comparison for the indicated strains grown on solid MM in the presence or absence of 200 mM $CaCl_2$ and/or 2 mM DTT at 30°C for 2.5 days. (D) Quantitative total conidial production for the strains shown in panel C. Error bars represent standard deviation from three replicates. Different lowercase letters on the bars of each group represent significant differences among strains (Tukey's multiple-comparison test, $P < 0.05$).

and conidiation on MM (2). The addition of 2 mM DTT on MM but not thermal stress aggravated the conidiation defects seen in the Δ*cnaA* mutant. Moreover, the conidiation defect was further aggravated in the Δ*clxA* Δ*cnaA* mutant, where conidium production was completely abolished on MM. In contrast to the Δ*cnaA* mutant, where extracellular $CaCl_2$ could restore the conidiation defects under DTT stress, this restoration was not seen in the Δ*cnaA* Δ*clxA* mutant (Fig. 4A and B; see Fig. S5 in the supplemental material).

We further tested the roles of *crzA*, which is one of the most well-known targets of calcineurin in fungi, in response to DTT and thermal stress (6, 7). The Δ*crzA* mutant is sensitive to DTT but not to thermal stress, which is consistent with the results from our Δ*cnaA* mutant. Hyphal radial growth and total conidium production in the Δ*crzA* mutant showed 24% ± 1.5% and 54% ± 7.1% reductions, respectively, on MM plus 2 mM DTT compared with cultures grown on MM alone. Moreover, the addition of DTT or thermal stress potentiated the defects seen in the Δ*crzA* Δ*clxA* mutant. However, both the Δ*crzA* and Δ*crzA* Δ*clxA* mutants exhibited extracellular calcium sensitivity (Fig. 4C and D; Fig. S5). Collectively, the above results indicated that calcineurin and its target gene, *crzA*, are involved in the fungal response to DTT stress. Moreover, restoration of DTT/thermal stress sensitivity in the Δ*clxA* mutant is calcineurin dependent.

Loss of *pmrA* abolishes extracellular calcium-based restoration of the DTT/thermal sensitivity in the Δ*clxA* mutant. Different stimuli can cause disruption of ER function, including calcium depletion from the ER lumen. The SPCA pump Pmr1 gene, which encodes a Ca^{2+}/Mn^{2+} P-type ATPase, has been shown to play a crucial role in replenishing Ca^{2+}-depleted organelles under ER stress (3, 23). Since the above results suggested that ClxA is involved in fungal ER stress adaptation, we hypothesized that ClxA and PmrA may coordinate the fungal ER stress response. To investigate the link between *clxA* and *pmrA*, we crossed the Δ*clxA* and Δ*pmrA* mutants. Consistent with our previous report (38), the Δ*pmrA* mutant showed a slight reduction in hyphal radial

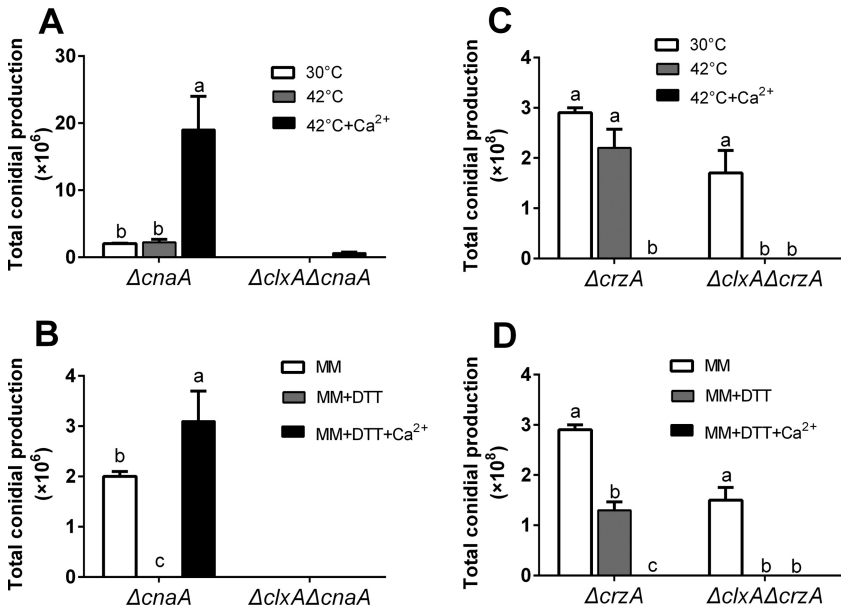

FIG 4 The DTT/thermal stress sensitivity in the Δ*clxA* mutant can be rescued by extracellular Ca^{2+} in a calcineurin-dependent way. (A and C) Quantitative total conidial production for the indicated strains grown on solid MM in the presence or absence of 200 mM $CaCl_2$ at 30 or 42°C for 2.5 days. (B and D) Quantitative total conidial production for the indicated strains grown on solid MM in the presence or absence of 200 mM $CaCl_2$ and/or 2 mM DTT at 30°C for 2.5 days. Different lowercase letters on the bars of each group represent significant differences among strains (Tukey's multiple-comparison test, $P < 0.05$).

growth and conidiation compared to the wild-type strain. Expectedly, the Δ*clxA* Δ*pmrA* double deletion mutant showed a further decrease in the hyphal radial growth and conidiation on MM compared to that seen in the single mutants (Fig. 5A and B). Moreover, thermal stress or the addition of 2 mM DTT to MM completely abolished conidiation in the Δ*clxA* Δ*pmrA* mutant. Importantly, in contrast to the Δ*clxA* mutant, where extracellular Ca^{2+} could restore the defects seen under DTT or thermal stress, this restoration was abolished in the Δ*clxA* Δ*pmrA* mutant (Fig. 5A to D). These results indicate that blocking Ca^{2+} entry into the ER by deletion of *pmrA* abolished extracellular calcium-based restoration of the DTT/thermal sensitivity in the Δ*clxA* mutant.

ClxA and MidA/CchA synergistically coordinate in response to extracellular calcium. Extracellular calcium restored the sensitivity to thermal/DTT stress in both the Δ*clxA* and Δ*midA* Δ*cchA* mutants. We hypothesized that *clxA* may be involved in intracellular calcium homeostasis. Consistent with this hypothesis, the Δ*clxA* mutant exhibited increased EGTA (calcium chelator) sensitivity compared to the parental strain (Fig. 6A and B). Moreover, phenotypic defects in hyphal radial growth and conidiation were exacerbated in the Δ*clxA* Δ*midA* Δ*cchA* mutant, especially in the presence of EGTA. Notably, growth retardation of the Δ*clxA* Δ*midA* Δ*cchA* mutant under low-calcium conditions was greatly reversed by the addition of 200 mM calcium to MM. These results suggested that ClxA and MidA/CchA are both required under the calcium-limiting conditions, but may have some nonoverlapping roles in maintaining intracellular calcium homeostasis.

To further explore the roles of ClxA in the transient $[Ca^{2+}]_c$, we monitored the extracellular calcium-induced changes in $[Ca^{2+}]_c$ in live *A. nidulans* wild-type and mutant cells in which codon-optimized aequorin was expressed. As shown in Fig. 6C and D, when treated with 100 mM $CaCl_2$, the $[Ca^{2+}]_c$ in parental wild-type cells transiently increased from a resting level of approximately 0.09 μM to a peak concentration of 0.9 μM. As expected, the Δ*midA* Δ*cchA* mutant showed a reduction of 37% $\pm$ 3.0% in the transient $[Ca^{2+}]_c$ under the same stimulation condition. Interestingly, the loss of *clxA* showed a reduction of 20% $\pm$ 2.2% in the transient $[Ca^{2+}]_c$. Moreover, the

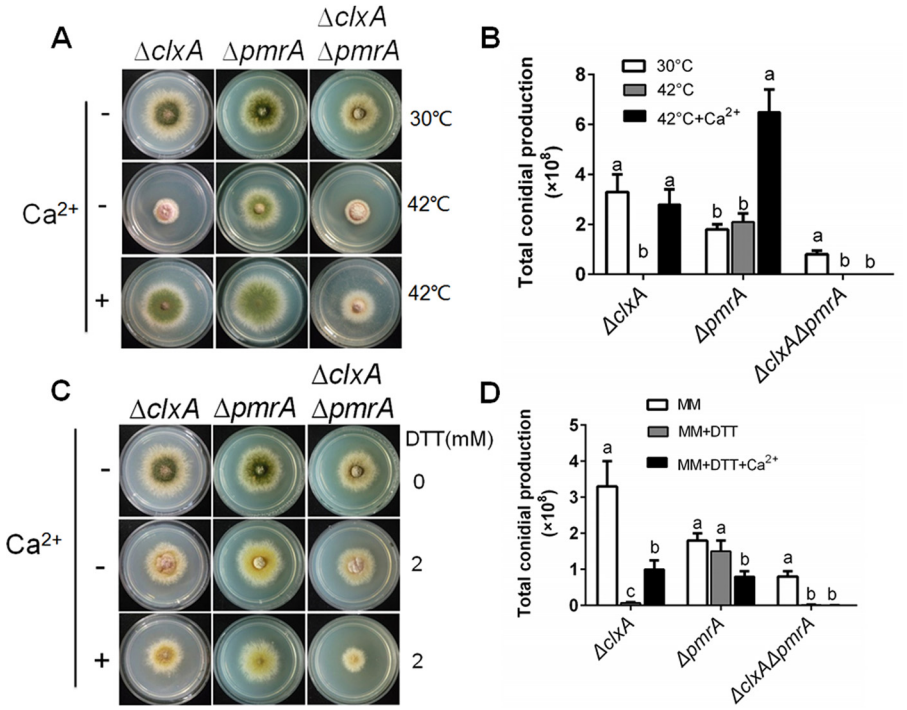

FIG 5 Loss of *pmrA* abolishes extracellular calcium-based restoration of the DTT/thermal sensitivity in the Δ*clxA* mutant. (A) Colony morphology comparison for the indicated strains grown on solid MM in the presence or absence of 200 mM $CaCl_2$ at 30 or 42°C for 2.5 days. (B) Quantitative total conidial production for the strains shown in panel A. (C) Colony morphology comparison for the indicated strains grown on solid MM in the presence or absence of 200 mM $CaCl_2$ and/or 2 mM DTT at 30°C for 2.5 days. (D) Quantitative total conidial production for the strains shown in panel C. Error bars represent standard deviations from three replicates. Different lowercase letters on the bars of each group represent significant differences among strains (Tukey's multiple-comparison test, $P < 0.05$).

Δ*clxA* Δ*midA* Δ*cchA* mutant exhibited a dramatic further reduction of 54% ± 4.2% in the transient $[Ca^{2+}]_c$ under the same stimulation condition. Those results suggested that ClxA and MidA/CchA complex synergistically coordinate the transient $[Ca^{2+}]_c$ in response to extracellular calcium.

ClxA mediates transient $[Ca^{2+}]_c$ in response to ER stress. Activation of the calcium signaling pathway is necessary for long-term survival of cells undergoing ER stress. The above results suggested that ClxA was involved in the transient $[Ca^{2+}]_c$ in response to extracellular calcium. To further explore the role of ClxA in mediating the transient $[Ca^{2+}]_c$ in response to ER stress, we measured the transient $[Ca^{2+}]_c$ in hyphal cells upon treatment with DTT after supplementation with EGTA to chelate extracellular calcium. As shown in Fig. 7A, after addition of 10 mM DTT to the medium, all strains responded with increased transient $[Ca^{2+}]_c$. However, the Δ*clxA* mutant exhibited a significantly lower increase in transient $[Ca^{2+}]_c$ compared to the parental wild-type strain. The transient $[Ca^{2+}]_c$ in the Δ*clxA* mutant was decreased to approximately 63% ± 6.1% of the parental wild-type strain under the same stimulation conditions.

As for all mammalian and *S. pombe* calnexins, ClxA has four repeats of the sequence KPEDWDE in the luminal domain, which have been reported to play a role in binding calcium and glucose (34, 35). To characterize the function of the luminal domain of ClxA in mediating the transient $[Ca^{2+}]_c$, a truncated *clxA* gene that contains the luminal domain of ClxA (*clxA*$^{\Delta c}$) was used to complement the Δ*clxA* mutant. As shown in Fig. 7B, when treated with 100 mM $CaCl_2$, the transient $[Ca^{2+}]_c$ in the *clxA*$^{\Delta c}$ mutant was similar to that in the Δ*clxA* mutant. In comparison, the transient $[Ca^{2+}]_c$ increased from 63% ± 6.1% in the Δ*clxA* mutant to 86% ± 4.2% in the *clxA*$^{\Delta c}$ mutant, compared to the reference strain after addition of 10 mM DTT to the medium (Fig. 7A). This suggested that the ClxA luminal domain plays a role in mediating transient $[Ca^{2+}]_c$ in response to

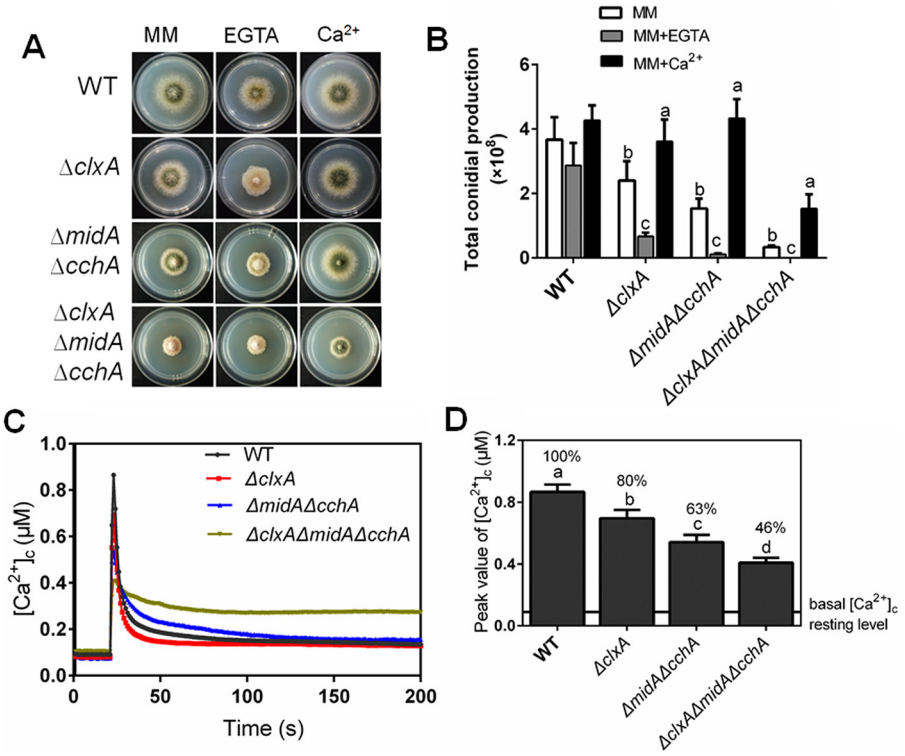

FIG 6 ClxA mediates transient $[Ca^{2+}]_c$ in response to extracellular calcium stimulus. (A) Colony morphology comparison for the indicated strains grown on solid MM in the presence or absence of 200 mM $CaCl_2$ or 2 mM EGTA at 30°C for 2.5 days. (B) Quantitative total conidial production for the strains shown in panel A. (C) Real-time monitoring of the $[Ca^{2+}]_c$ of indicated strains following a stimulus with 100 mM $CaCl_2$. (D) The peak of transient $[Ca^{2+}]_c$ of the indicated strains after treatment with 100 mM $CaCl_2$. Error bars represent standard deviations from three replicates. Different lowercase letters on the bars of each group represent significant differences among strains (Tukey's multiple-comparison test, $P < 0.05$).

ER stress but not to extracellular calcium stimulus. Furthermore, the conidiation and hyphal radial growth defects of the Δ*clxA* mutant were completely restored under DTT and partially restored under thermal stress by complementation with the luminal domain (Fig. 7C and D). Taken together, these results suggest that ClxA, in particular its luminal domain, plays a role in mediating the transient $[Ca^{2+}]_c$ in response to ER stress in the absence of extracellular calcium.

DISCUSSION

The results presented herein show that ClxA, a molecular chaperone located in the ER, plays crucial roles in regulating $[Ca^{2+}]_c$ homeostasis in *A. nidulans*. Consistent with its role as a molecular chaperone in glycoprotein folding and quality control in the ER, calnexin null mutants of several fungi show sensitivity to many adverse environmental conditions that cause protein misfolding, including high temperature, nutrient limitation, or cation depletion (39, 40). Importantly, we found that the addition of calcium could dramatically restore the sensitivity seen in the Δ*clxA* mutant under ER stress induced by high temperature or DTT. Moreover, the Δ*clxA* mutant exhibited markedly reduced conidium formation and hyphal growth defects under low-calcium conditions, which are similar to defects caused by mutations in the HACS components MidA and CchA (14). All the above results support the notion that *clxA* is involved in calcium sequestration or regulation in *A. nidulans*.

To further explore the role of *clxA* in $[Ca^{2+}]_c$ regulation, we monitored transient $[Ca^{2+}]_c$ in response to stimuli in real time. The transient $[Ca^{2+}]_c$ in the Δ*clxA* mutant was lower (approximately 20% lower) than that in the parental wild-type control following treatment with a high-extracellular-calcium stress stimulus, suggesting that the loss of *clxA* reduced calcium influx into the cytoplasm. Moreover, the Δ*clxA* Δ*midA* Δ*cchA* triple

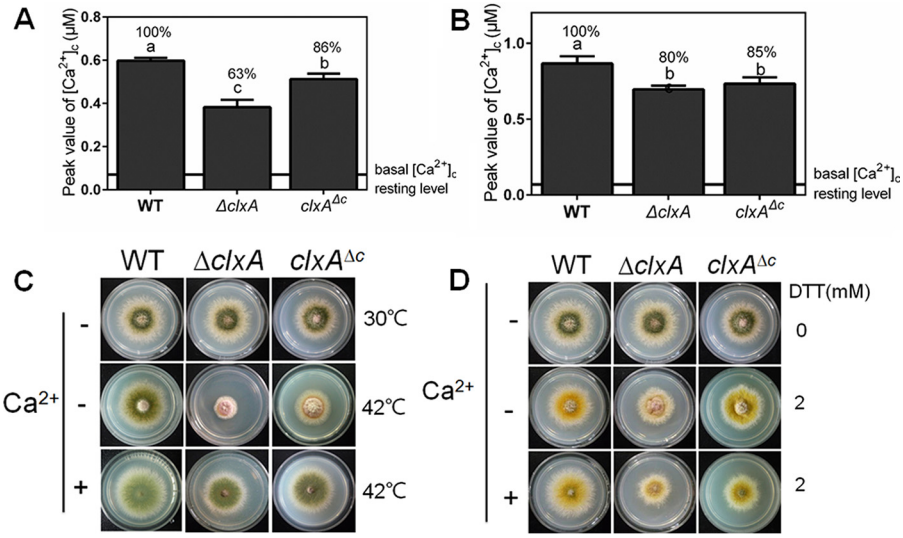

FIG 7 ClxA mediates transient $[Ca^{2+}]_c$ in response to ER stress. (A) The peak of transient $[Ca^{2+}]_c$ of the indicated strains after treatment with EGTA and DTT. (B) The peak of transient $[Ca^{2+}]_c$ of the indicated strains after treatment with 100 mM $CaCl_2$. Error bars represent standard deviations from three replicates. Different lowercase letters on the bars of each group represent significant differences among strains (Tukey's multiple comparison test, $P < 0.05$). (C) Colony morphology comparison for the indicated strains grown on solid MM in the presence or absence of 200 mM $CaCl_2$ at 30 or 42°C for 2.5 days. (D) Colony morphology comparison for the indicated strains grown on solid MM in the presence or absence of 200 mM $CaCl_2$ and/or 2 mM DTT at 30°C for 2.5 days.

mutant had a further decreased transient $[Ca^{2+}]_c$ than the Δ*clxA* single mutant under the same stimulation condition, suggesting that *clxA* may have a different function from that of the MidA/CchA complex in transient $[Ca^{2+}]_c$. The transient increase in $[Ca^{2+}]_c$ may be the result of uptake from the extracellular environment or release from intracellular calcium stores. We further tested the transient $[Ca^{2+}]_c$ of EGTA-pretreated cells in response to DTT stimulation. As expected, when calcium influx from the extracellular environment was blocked by the addition of EGTA, the transient $[Ca^{2+}]_c$ in the Δ*clxA* mutant was also decreased (approximately 30%) compared to that in the reference strain in response to DTT treatment. These data suggested that ClxA mediates the release of intracellular calcium stores under ER stress in the absence of extracellular calcium. Considering the location of the ER, ClxA may mediate Ca^{2+} release from the ER, a reservoir of Ca^{2+} primarily mobilized for signaling (25, 41).

ER stress can promote prolonged depletion of calcium that will lead to cell death. To offset the detrimental effects of Ca^{2+} efflux, most cells employ a regulatory mechanism known as capacitative calcium entry (CCE), which stimulates Ca^{2+} influx specifically in response to the removal of Ca^{2+} from the ER (26, 42). The evidence to date has shown that a high-affinity Ca^{2+} influx channel composed of Cch1/Mid1 allows calcium influx across the plasma membrane, which helps replenish the depleted organelles under ER stress (25, 26, 43). Furthermore, Pmr1, which localizes primarily to the Golgi complex of *S. cerevisiae*, supplies the majority of the Ca^{2+} and Mn^{2+} to the ER and Golgi complex. The loss of *pmr1* also activates HACS (3, 19, 44). Thus, *cch1*/*mid1* and *pmr1* all appear to function within a signaling pathway that promotes the acquisition and concentration of essential Ca^{2+} into secretory organelles, which closely parallels the CCE pathway of animal cells (26). As mentioned above, the addition of calcium restored the defects seen in the Δ*clxA* mutant under ER stress, and we thought that the addition of calcium may be able to replenish the Ca^{2+}-depleted ER in the Δ*clxA* mutant under ER stress. To test our hypothesis, we constructed a Δ*clxA* Δ*midA* Δ*cchA* mutant and a Δ*clxA* Δ*pmrA* mutant. As expected, when Ca^{2+} entry into the ER was blocked by the deletion of *midA*/*cchA* or *pmrA*, the calcium-based restoration seen in the Δ*clxA* mutant was abolished. Collectively, these results suggested that ClxA may cooperate with MidA/CchA and PmrA to maintain ER Ca^{2+} homeostasis under ER stress.

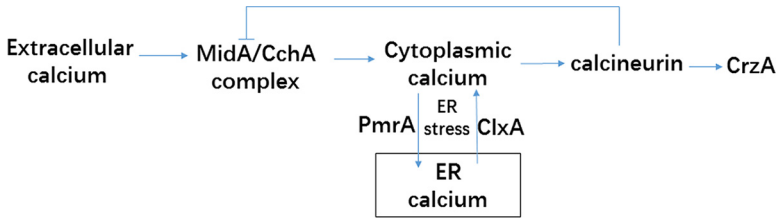

FIG 8 A working model of how ClxA function regulates $[Ca^{2+}]_c$ homeostasis in *A. nidulans*. ClxA coordinates with MidA/CchA to regulate $[Ca^{2+}]_c$ homeostasis in response to extracellular calcium stimulus. ClxA regulates $[Ca^{2+}]_c$ homeostasis in response to ER stress in the absence of extracellular calcium.

The regulation of ions in the ER is of central importance to the cell, given the numerous functions of this organelle. Recently, we reported that AkrA, a putative palmitoyl transferase in *A. nidulans*, mediates calcium influx by a DHHC (Asp-His-His-Cys)-dependent mechanism, performing an essential role in calcium homeostasis and allowing cells to survive high extracellular calcium, ER, and plasma membrane stress conditions. The loss of AkrA completely abolishes transient increase in $[Ca^{2+}]_c$ in response to ER stress in the absence of extracellular calcium, suggesting palmitoylation plays an important role in mediating calcium release from intracellular stores in response to ER stress (17). Interestingly, the mammalian protein calnexin can switch its roles between quality control and ER Ca^{2+} signaling through palmitoylation. Palmitoylated calnexin interacts with sarcoplasmic/endoplasmic reticulum ATPase (SERCA2b), which determines ER $[Ca^{2+}]$ and the regulation of ER-mitochondria Ca^{2+} cross talk. In contrast, nonpalmitoylated calnexin interacts with the oxidoreductase ERp57 and performs its well-known function in ER quality control (45). However, SERCA pumps are absent in organisms such as fungi. Thus, it is likely that a more widely conserved p-type ATPase in the ER, such as Cod1p/spf1p or Cta4p is responsible for ER ion maintenance in fungi (46, 47). It is possible ClxA interacts with an alternative ATPase in the ER to regulate ER Ca^{2+} homeostasis. However, ClxA contains four conserved motifs in its lumen, which have been proven to be involved in Ca^{2+} binding in both yeast and mammalian cells. Our data showed that this domain is crucial for the restoration of the transient $[Ca^{2+}]_c$ increases in response to ER stress. Thus, ClxA itself may also act as a calcium-binding protein to buffer Ca^{2+} in the ER.

In conclusion, our results provide the report that ClxA, an ER located chaperone plays an important role in the regulation of Ca^{2+} homeostasis in fungi. We further provide evidence that ClxA cooperates with the conserved calcium signaling pathway components MidA/CchA, calcineurin, and PmrA in fungal ER stress adaptation. A putative working model of this mechanism is presented in Fig. 8. Our results expand knowledge of the function of calnexin and mechanisms of fungal stress adaptation.

MATERIALS AND METHODS

Strains, media, and cultural conditions. All *A. nidulans* strains used in this study are listed in Table 1. TN02A7, a strain with deletion of a gene required for nonhomologous end joining in double-strand break repair (48), was used in all transformation experiments as a reference strain. All fungal strains were routinely cultured on minimal medium (MM) with nutrition supplements to support the growth of relevant auxotrophic strains as described previously (49).

Genetic mutant strain construction. To generate constructs for the Δ*clxA* strain, the double-joint PCR method was used as previously described (50). In brief, a 932-bp 5′-flank DNA fragment and a 1,081-bp 3′-flank DNA fragment were amplified from genomic DNA (gDNA) of *A. nidulans* reference strain TN02A7 using the primers P1/P3 and P4/P6, respectively. The *Aspergillus fumigatus pyrG* gene, used as a selectable nutritional marker for transformation, was amplified from the plasmid pXDRFP4 (Fungal Genetics Stock Center) using the primer pair *AfpyrG*F/*AfpyrG*R. The linearized DNA fragment, including a 5′ flank of *clxA*, *pyrG*, and a 3′ flank of *clxA*, was amplified with primer pair P2/P5. The final fusion PCR product was purified and transformed into TN02A7. A diagnostic PCR assay was performed to detect *clxA* replaced by *A. fumigatus pyrG* (*AfpyrG*) at the original *clxA* locus using primer pairs P1/*AfpyrG*R, *AfpyrG*F/P6, and *clxA*(S)/*clxA*(R), respectively. Furthermore, reverse transcription-PCR (RT-PCR) was performed to confirm the deletion of the *clxA* gene at transcriptional level using primer pair RT*clxA*F/RT*clxA*R. The same strategy was used to construct the *crzA* deletion (Δ*crzA*) strain. To complement the Δ*clxA* strain,

TABLE 1 Characteristics of all *A. nidulans* strains used in this study

Strain name	Deleted and labeled gene(s)[a]	Genotype	Source or reference
TN02A7	Parental wild-type strain	*pyrG89 pyroA4 nkuA::argB riboB2 veA1*	FGSC
ZSA01	Δ*midA* Δ*cchA*	*pyrG89* Δ*midA::pyroA pyroA nkuA::argB2* Δ*cchA::pyrG riboB2 veA1*	14
ZSA02	Δ*cnaA*	Δ*cnaA::pyrG nkuA::argB2 riboB2 veA1*	51
ZSA03	Δ*pmrA*	*pyrG89 pyroA4 nkuA::argB2* Δ*pmrA::pyroA riboB2 veA1*	38
ZSA04	Δ*clxA*	*pyrG89 pyroA4 nkuA::argB2* Δ*clxA::pyrG riboB2 veA1*	This study
ZSA05	*clxA*::Δ*clxA*	*pyrG89 pyroA4 nkuA::argB2* Δ*clxA::pyrG riboB2 veA1 clxA::pyroA*	This study
ZSA06	Δ*clxA* Δ*midA* Δ*cchA*	*pyrG89* Δ*midA::pyroA pyroA* Δ*clxA::pyrG nkuA::argB2* Δ*cchA::pyrG riboB2 veA1*	This study
ZSA07	Δ*clxA* Δ*cnaA*	*nkuA::argB* Δ*clxA::pyrG* Δ*cnaA::pyrG riboB2 veA1*	This study
ZSA08	Δ*crzA*	*pyrG89 pyroA4 nkuA::argB2* Δ*crzA::pyroA riboB2 veA1*	This study
ZSA09	Δ*clxA* Δ*crzA*	*pyrG89 pyroA4 nkuA::argB2* Δ*clxA::pyrG* Δ*crzA::pyroA riboB2 veA1*	This study
ZSA10	Δ*clxA* Δ*pmrA*	*pyrG89 pyroA4 nkuA::argB2* Δ*clxA::pyrG* Δ*pmrA::pyroA riboB2 veA1*	This study
ZSA11	ClxA-GFP	*pyrG89 pyroA4 nkuA::argB2 clxA::GFP::pyr4 riboB2*; *veA1*	This study
ZSA12	TN02A7-AEQ	*pyrG89 nkuA::argB2 riboB2 veA1* pAEQ-aeqS	This study
ZSA13	Δ*clxA*-AEQ	*pyrG89* Δ*clxA::pyrG nkuA::argB2 riboB2 veA1* pAEQ-aeqS	This study
ZSA14	Δ*clxA* Δ*midA* Δ*cchA*-AEQ	*pyrG89* Δ*clxA::pyrG* Δ*midA::pyroA* Δ*cchA::pyrG nkuA::argB2 veA1* pAEQ-aeqS	This study
ZSA15	$clxA^{\Delta c}$	*pyrG89* Δ*clxA::*$clxA^{\Delta c}$*::pyroA nkuA::argB2 riboB2 veA1*	This study
ZSA16	$clxA^{\Delta c}$-AEQ	*pyrG89* Δ*clxA::*$clxA^{\Delta c}$*::pyroA nkuA::argB2 riboB2 veA1* pAEQ-aeqS	This study

[a]AEQ, aequorin.

a 4,061-bp fragment, which includes a 1,811-bp promoter region, a 1,901-bp coding sequence, and the 3′ flank of the *clxA* gene, was amplified from TN02A7 with primer pair Rec*lxA*P1/Rec*lxA*P3. The selectable nutritional marker *pyroA* was amplified from the plasmid pQa-pyroA with primer pair *pyroA*F/*pyroA*R, and then the two fragments were fused together by PCR with primer pair Re*clxA*P2/*pyroA*R. The resulting fusion products were transformed to the Δ*clxA* strain. To complement the Δ*clxA* strain with its luminal domain, the fragment including a promoter sequence and a luminal domain of *clxA* and the fragment including the 3′ terminator of *clxA* were amplified with primer pairs *clxAL*P1/*clxAL*P3 and *clxAL*P4/*clxAL*P5, respectively, and then the two fragments and the selective marker gene *pyroA* were fused together by PCR with primers *clxAL*P2/*pyroA*R1. The resulting fusion products were transformed to the Δ*clxA* strain. To construct the Δ*clxA* Δ*midA* Δ*cchA*, Δ*clxA* Δ*cnaA*, Δ*clxA* Δ*crzA*, and Δ*clxA* Δ*pmrA* mutants, the Δ*clxA* strain was crossed with the Δ*midA* Δ*cchA* (14), Δ*cnaA* (51), and Δ*pmrA* (38) mutants, respectively. All progeny were screened according to a standard protocol (49).

To localize ClxA, a *gfp-pyrG* fragment was amplified from plasmid pFNO3 using primer pair *GFPAf-pyrGF*/*GFPAfpyrG*R. The same approach as that described previously (48) was used to construct the ClxA-GFP fusion cassette. In brief, a 1,451-bp fragment immediately upstream of the *clxA* stop codon and a 1,426-bp fragment immediately downstream of the *clxA* stop codon were amplified from strain TN02A7 using primer pairs *GFPclxA*P1/*GFPclxA*P3 and *GFPclxA*P4/*GFPclxA*P6, respectively. The ClxA-GFP fusion PCR cassette (using primer pair *GFPclxA*P2/*GFPclxA*P5) was transformed into strain TN02A7, and the transformants embedding homologous integration were verified by PCR using primer pair *GFPclxA*P1/*GFPAf-pyrG*R.

For generation of aequorin-expressing *A. nidulans* strains, the plasmid pAEQS1-15 containing codon-optimized aequorin, and selective marker *pyroA* or *riboB* genes were cotransformed into the indicated strains. Transformants were screened for aequorin expression using methods described previously (52), and high-aequorin-expressing strains were selected after homokaryon purification involving repeated plating of single conidia. All transformation was performed as previously described (53). The primers for the genetic mutant strains construction are listed in Table 2.

Microscopic observation and image processing. To visualize localization of ClxA-GFP, conidia of ClxA-GFP strain were inoculated onto precleaned glass coverslips overlaid with liquid media at 37°C for 12 h. DNA was stained using 4′,6-diamidino-2-phenylindole (DAPI). Differential interference contrast (DIC) and fluorescent images of the cells were collected with a Zeiss Axio Imager A1 microscope (Zeiss, Jena, Germany). These images were then collected and analyzed by a SensiCam QE cooled digital camera system (Cooke Corporation, Germany) with the MetaMorph/MetaFluor combination software package (Universal Imaging, West Chester, PA).

Western blotting. Western blotting was performed as previously described (54). In brief, conidia from the ClxA-GFP strain were inoculated in liquid MM and then shaken at 220 rpm on a rotary shaker at 37°C for 24 h, and the mycelium was collected, ground in liquid nitrogen, and suspended in ice-cold extraction buffer (50 mM HEPES [pH 7.4], 137 mM KCl, 10% glycerol, 1 mM EDTA, 1 μg/ml pepstatin A, 1 μg/ml leupeptin, 1 mM phenylmethylsulfonyl fluoride [PMSF]). Forty micrograms of protein was subjected to 10% SDS-PAGE and then transferred to a polyvinylidene difluoride (PVDF) membrane (Immobilon-P; Millipore) in a mixture of 384 mM glycine, 50 mM Tris (pH 8.4), and 20% methanol at 250 mA for 1.5 h. Next, the membrane was probed sequentially with 1:3,000 dilutions of anti-GFP and goat anti-rabbit IgG-horseradish peroxidase diluted in a mixture of phosphate-buffered saline (PBS), 5% milk, and 0.3% Tween 20, and the blot was developed by chemiluminescence (ECL; Amersham).

Plate assays. To assess the influence of thermal stress on the fungal growth, wild-type and relevant strains were cultured at 42 or 30°C, respectively, for 2.5 days. The influence of DTT stress on fungal growth was tested by addition of 2 mM DTT to the minimal medium. To assess the role of calcium ion on fungal growth, 200 mM $CaCl_2$ was added to MM. Two microliters of conidia from the stock (1×10^7

TABLE 2 Primers used in this study

Primer	Sequence (5′→3′)
ClxA-GFP	
*GFPclxA*P1	TATGAGGTCAAGCCGCAAAG
*GFPclxA*P2	CCTTGTTGGAACTGACGCAT
*GFPclxA*P3	CCAGCGCCTGCACCAGCTCCCTCCGCAGACGATCGGGTGGT
*GFPclxA*P4	CATCAGTGCCTCCTCTCAGACAGTAAGACCAGTATGAGTGAAAAGAGC
*GFPclxA*P5	GCCGACTAAAGGAGTTTGTGA
*GFPclxA*P6	ACGGGTGACGAGGTTATTGG
*GFPAfpyrG*F	GGAGCTGGTGCAGGCGCTGG
*GFPAfpyrG*R	CTGTCTGAGAGGAGGCACTGATG
clxA deletion	
P1	CAGGGAAATTCGCAAAAGAAC
P2	GAGGATGTGACGAGGTGAGTG
P3	GGTGAAGAGCATTGTTTGAGGCAGAGACCAAAGCGGAGGTAAGAG
P4	CATCAGTGCCTCCTCTCAGACAGCATTATTGTTGGTGCCATCGG
P5	GTATCGCCTCAGGAACGCTTA
P6	CAGGGGATGGAATGGTAAAGAC
clxA(S)	TATGAGGTCAAGCCGCAAAG
clxA(A)	TTAGGGACAGTGGGAGGAATC
RT*clxA*F	CTCCCTTGTTTGTGGTGGTGC
RT*clxA*R	GTCAGGAATGCTGTTCGGCTC
*AfpyrG*F	GCCTCAAACAATGCTCTTCACC
*AfpyrG*R	CTGTCTGAGAGGAGGCACTGATG
clxA reconstituted	
Re*clxA*P1	TCCCCATCTATTTGACCC
Re*clxA*P2	ACACGAATGTGGTTTGGGAG
Re*clxA*P3	CTATTATCTGACTTACCCGCCAACCAACTCTTTCCCAACCCGTG
*pyroA*F	TTGGCGGGTAAGTCAGATAATAG
*pyroA*R	CTGACTTGACGCTTTCTCTTGG
crzA deletion	
*crzA*P1	CAGCAAAAGCCGCCAGTT
*crzA*P2	TGTGCGGAATGCCCAGAT
*crzA*P3	CTATTATCTGACTTACCCGCCAAGGCAAAGAGCTATGCAGACAAGA
*crzA*P4	CCAAGAGAAAGCGTCAAGTCAG CACATCTTTTGCATCCCTTTG
*crzA*P5	AAACAACCCGCACCCCTAC
*crzA*P6	GCATTCGCTGTGGCATTCT
crzA(S)	TCGATTTCTCGCTCTACCAGG
crzA(R)	TGAAGCAGCCAAAGCGTCTA
$clxA^{\Delta c}$ construction	
*clxAL*P1	AGGATGTGACGAGGTGAGTGAG
*clxAL*P2	CCTTACGGGCGAAGCAAT
*clxAL*P3	AGGCTCTTTTCACTCATACTGGTCTTACTCGGGAACCTGCTTGAC
*clxAL*P4	GACCAGTATGAGTGAAAAGAGCCT
*clxAL*P5	CTATTATCTGACTTACCCGCCAAATCGCCTCAGGAACGCTTA
*pyroA*R1	GCATTCCGCTTCTTCCAAGT
RT-PCR	
*brlA*RTF	GGGCCATACGGAGTCGATTG
*brlA*RTR	GGCGAGTGCGTCTTGAAGGT
*tub*RTF	TTCCGTCCCGACAACTTCGT
*tub*RTR	TCACAGCCTTCAGCCTCACG

conidia/ml) of indicated strains was spotted onto relevant media, and then the colonies were observed and imaged, and the total conidial production of each colony was counted. For each experiment, at least three replicate plates were used to test the phenotypes for each strain.

Quantitative real-time PCR analysis. Total RNA was isolated using TRIzol (Invitrogen) following the manufacturer's instruction. Reverse transcription-PCR (RT-PCR) was carried out using HiScript QRT SuperMix (Vazyme), and then cDNA was used for the real-time analysis, which was performed using an ABI one-step fast thermocycler (Applied Biosystems), and the reaction products were detected with SYBR Premix *Ex Taq* (TaKaRa). Transcript levels were calculated by determining the comparative change in cycle threshold and normalized against the expression of the *A. nidulans* tubulin gene.

Intracellular Ca^{2+} measurement. The cytoplasmic Ca^{2+} concentrations were determined by a previously described method (17, 55). In brief, 1×10^7 spores/ml of strains expressing the codon-

optimized aequorin gene were cultured in liquid MM and were distributed into each well of a 96-well microtiter plate (100 μl/well). Six wells were used in parallel for each treatment. The plates were incubated at 37°C for 18 h, and then the medium was removed and the plates were rinsed twice with PGM (20 mM PIPES [pH 6.7], 50 mM glucose, 1 mM $MgCl_2$). Aequorin was reconstituted by incubating mycelia in 100 μl PGM containing 2.5 μM coelenterazine N (Sigma-Aldrich) for 4 h at 4°C in the dark. Then, the liquid was removed, and the plates were rinsed twice with PGM again. Plates were reconstituted with 100 μl PGM by incubating mycelia at room temperature for 1 h. To chelate extracellular Ca^{2+}, 1 mM EGTA was added to each well for 10 min prior to stimulus injection. Following recovery, luminescence was measured for 180 s after 100 mM $CaCl_2$ or 10 mM DTT addition within 20 s. At the end of each experiment, the active aequorin was completely discharged by permeabilizing the cells with 20% (vol/vol) ethanol in the presence of 3 M $CaCl_2$. Luminescence was measured with an LB 96P MicroLumat luminometer (Berthold Technologies, Germany). The data from relative light unit (RLU) values detected were converted into $[Ca^{2+}]_c$ by using the empirically derived calibration formula pCa = 0.332588 ($-\log k$) + 5.5593, where k is luminescence (RLU) s^{-1}/total luminescence (RLU) and pCa is $-\log[Ca^{2+}]$ (52). Error bars represent the standard error of the mean from six independent experiments, and percentages in the figures represent peak of $[Ca^{2+}]_c$ compared to that of the wild-type (100%).

SUPPLEMENTAL MATERIAL

Supplemental material for this article may be found at https://doi.org/10.1128/AEM.00673-17.

SUPPLEMENTAL FILE 1, PDF file, 0.6 MB.

ACKNOWLEDGMENTS

This work was financially supported by grants from the National Natural Science Foundation of China (NSFC31470193 and NSFC31200057) to Shizhu Zhang, the priority academic program development (PAPD) of Jiangsu Higher Education Institutions, and the National Natural Science Foundation of China (NSFC31400065) to Sha Wang.

We thank N. D. Read (University of Manchester) for kindly providing plasmid pAEQS1-15, G. H. Goldman (Universidade de São Paulo) for the *A. nidulans cnaA* deletion strain, and H. M. Park (Chungnam National University) for plasmid pQa-pyroA.

REFERENCES

1. Juvvadi PR, Lamoth F, Steinbach WJ. 2014. Calcineurin as a multifunctional regulator: unraveling novel functions in fungal stress responses, hyphal growth, drug resistance, and pathogenesis. Fungal Biol Rev 28:56–69. https://doi.org/10.1016/j.fbr.2014.02.004.
2. Wang S, Liu X, Qian H, Zhang S, Lu L. 2016. Calcineurin and calcium channel CchA coordinate the salt stress response by regulating cytoplasmic Ca^{2+} homeostasis in Aspergillus nidulans. Appl Environ Microbiol 82:3420–3430. https://doi.org/10.1128/AEM.00330-16.
3. Cunningham KW. 2011. Acidic calcium stores of Saccharomyces cerevisiae. Cell Calcium 50:129–138. https://doi.org/10.1016/j.ceca.2011.01.010.
4. Cyert MS. 2001. Genetic analysis of calmodulin and its targets in Saccharomyces cerevisiae. Annu Rev Genet 35:647–672. https://doi.org/10.1146/annurev.genet.35.102401.091302.
5. Stathopoulos AM, Cyert MS. 1997. Calcineurin acts through the CRZ1/TCN1-encoded transcription factor to regulate gene expression in yeast. Genes Dev 11:3432–3444. https://doi.org/10.1101/gad.11.24.3432.
6. Matheos DP, Kingsbury TJ, Ahsan US, Cunningham KW. 1997. Tcn1p/Crz1p, a calcineurin-dependent transcription factor that differentially regulates gene expression in Saccharomyces cerevisiae. Genes Dev 11:3445–3458. https://doi.org/10.1101/gad.11.24.3445.
7. Karababa M, Valentino E, Pardini G, Coste AT, Bille J, Sanglard D. 2006. CRZ1, a target of the calcineurin pathway in Candida albicans. Mol Microbiol 59:1429–1451. https://doi.org/10.1111/j.1365-2958.2005.05037.x.
8. Clapham DE. 2007. Calcium signaling. Cell 131:1047–1058. https://doi.org/10.1016/j.cell.2007.11.028.
9. Berridge MJ, Bootman MD, Roderick HL. 2003. Calcium signalling: dynamics, homeostasis and remodelling. Nat Rev Mol Cell Biol 4:517–529. https://doi.org/10.1038/nrm1155.
10. Muller EM, Locke EG, Cunningham KW. 2001. Differential regulation of two Ca^{2+} influx systems by pheromone signaling in Saccharomyces cerevisiae. Genetics 159:1527–1538.
11. Groppi S, Belotti F, Brandao RL, Martegani E, Tisi R. 2011. Glucose-induced calcium influx in budding yeast involves a novel calcium transport system and can activate calcineurin. Cell Calcium 49:376–386. https://doi.org/10.1016/j.ceca.2011.03.006.
12. Muller EM, Mackin NA, Erdman SE, Cunningham KW. 2003. Fig1p facilitates Ca^{2+} influx and cell fusion during mating of Saccharomyces cerevisiae. J Biol Chem 278:38461–38469. https://doi.org/10.1074/jbc.M304089200.
13. Zhang S, Zheng H, Long N, Carbo N, Chen P, Aguilar PS, Lu L. 2014. FigA, a putative homolog of low-affinity calcium system member Fig1 in Saccharomyces cerevisiae, is involved in growth and asexual and sexual development in Aspergillus nidulans. Eukaryot Cell 13:295–303. https://doi.org/10.1128/EC.00257-13.
14. Wang S, Cao J, Liu X, Hu H, Shi J, Zhang S, Keller NP, Lu L. 2012. Putative calcium channels CchA and MidA play the important roles in conidiation, hyphal polarity and cell wall components in Aspergillus nidulans. PLoS One 7:e46564. https://doi.org/10.1371/journal.pone.0046564.
15. Paidhungat M, Garrett S. 1997. A homolog of mammalian, voltage-gated calcium channels mediates yeast pheromone-stimulated Ca^{2+} uptake and exacerbates the cdc1(Ts) growth defect. Mol Cell Biol 17:6339–6347. https://doi.org/10.1128/MCB.17.11.6339.
16. Harren K, Tudzynski B. 2013. Cch1 and Mid1 are functionally required for vegetative growth under low-calcium conditions in the phytopathogenic ascomycete Botrytis cinerea. Eukaryot Cell 12:712–724. https://doi.org/10.1128/EC.00338-12.
17. Zhang Y, Zheng Q, Sun C, Song J, Gao L, Zhang S, Munoz A, Read ND, Lu L. 2016. Palmitoylation of the cysteine residue in the DHHC motif of a palmitoyl transferase mediates Ca^{2+} homeostasis in Aspergillus. PLoS Genet 12:e1005977. https://doi.org/10.1371/journal.pgen.1005977.
18. Patel S, Docampo R. 2010. Acidic calcium stores open for business: expanding the potential for intracellular Ca^{2+} signaling. Trends Cell Biol 20:277–286. https://doi.org/10.1016/j.tcb.2010.02.003.
19. Strayle J, Pozzan T, Rudolph HK. 1999. Steady-state free Ca^{2+} in the yeast endoplasmic reticulum reaches only 10 μM and is mainly controlled by the secretory pathway pump pmr1. EMBO J 18:4733–4743. https://doi.org/10.1093/emboj/18.17.4733.
20. Bonilla M, Nastase KK, Cunningham KW. 2002. Essential role of calcineurin in response to endoplasmic reticulum stress. EMBO J 21:2343–2353. https://doi.org/10.1093/emboj/21.10.2343.

21. MacLennan DH, Rice WJ, Green NM. 1997. The mechanism of Ca^{2+} transport by sarco(endo)plasmic reticulum Ca^{2+}-ATPases. J Biol Chem 272:28815–28818. https://doi.org/10.1074/jbc.272.46.28815.
22. Carafoli E, Brini M. 2000. Calcium pumps: structural basis for and mechanism of calcium transmembrane transport. Curr Opin Chem Biol 4:152–161. https://doi.org/10.1016/S1367-5931(99)00069-1.
23. Durr G, Strayle J, Plemper R, Elbs S, Klee SK, Catty P, Wolf DH, Rudolph HK. 1998. The medial-Golgi ion pump Pmr1 supplies the yeast secretory pathway with Ca^{2+} and Mn^{2+} required for glycosylation, sorting, and endoplasmic reticulum-associated protein degradation. Mol Biol Cell 9:1149–1162. https://doi.org/10.1091/mbc.9.5.1149.
24. Hogan PG, Rao A. 2007. Dissecting ICRAC, a store-operated calcium current. Trends Biochem Sci 32:235–245. https://doi.org/10.1016/j.tibs.2007.03.009.
25. Hong MP, Vu K, Bautos J, Gelli A. 2010. Cch1 restores intracellular Ca^{2+} in fungal cells during endoplasmic reticulum stress. J Biol Chem 285:10951–10958. https://doi.org/10.1074/jbc.M109.056218.
26. Locke EG, Bonilla M, Liang L, Takita Y, Cunningham KW. 2000. A homolog of voltage-gated Ca^{2+} channels stimulated by depletion of secretory Ca^{2+} in yeast. Mol Cell Biol 20:6686–6694. https://doi.org/10.1128/MCB.20.18.6686-6694.2000.
27. Wada I, Rindress D, Cameron PH, Ou WJ, Doherty JJ, II, Louvard D, Bell AW, Dignard D, Thomas DY, Bergeron JJ. 1991. SSR alpha and associated calnexin are major calcium binding proteins of the endoplasmic reticulum membrane. J Biol Chem 266:19599–19610.
28. Michalak M, Robert Parker JM, Opas M. 2002. Ca^{2+} signaling and calcium binding chaperones of the endoplasmic reticulum. Cell Calcium 32:269–278. https://doi.org/10.1016/S0143416002001884.
29. Xu X, Azakami H, Kato A. 2004. P-domain and lectin site are involved in the chaperone function of Saccharomyces cerevisiae calnexin homologue. FEBS Lett 570:155–160. https://doi.org/10.1016/j.febslet.2004.06.039.
30. Rutkevich LA, Williams DB. 2011. Participation of lectin chaperones and thiol oxidoreductases in protein folding within the endoplasmic reticulum. Curr Opin Cell Biol 23:157–166. https://doi.org/10.1016/j.ceb.2010.10.011.
31. Ruddock LW, Molinari M. 2006. N-glycan processing in ER quality control. J Cell Sci 119:4373–4380. https://doi.org/10.1242/jcs.03225.
32. Lamriben L, Graham JB, Adams BM, Hebert DN. 2016. N-Glycan-based ER molecular chaperone and protein quality control system: the calnexin binding cycle. Traffic 17:308–326. https://doi.org/10.1111/tra.12358.
33. Williams DB. 2006. Beyond lectins: the calnexin/calreticulin chaperone system of the endoplasmic reticulum. J Cell Sci 119:615–623. https://doi.org/10.1242/jcs.02856.
34. Parlati F, Dignard D, Bergeron JJ, Thomas DY. 1995. The calnexin homologue $cnx1^+$ in Schizosaccharomyces pombe, is an essential gene which can be complemented by its soluble ER domain. EMBO J 14:3064–3072.
35. Baksh S, Michalak M. 1991. Expression of calreticulin in Escherichia coli and identification of its Ca^{2+} binding domains. J Biol Chem 266:21458–21465.
36. de Virgilio C, Burckert N, Neuhaus JM, Boller T, Wiemken A. 1993. CNE1, a Saccharomyces cerevisiae homologue of the genes encoding mammalian calnexin and calreticulin. Yeast 9:185–188. https://doi.org/10.1002/yea.320090209.
37. Parlati F, Dominguez M, Bergeron JJ, Thomas DY. 1995. Saccharomyces cerevisiae CNE1 encodes an endoplasmic reticulum (ER) membrane protein with sequence similarity to calnexin and calreticulin and functions as a constituent of the ER quality control apparatus. J Biol Chem 270:244–253. https://doi.org/10.1074/jbc.270.1.244.
38. Jiang H, Liu F, Zhang S, Lu L. 2014. Putative PmrA and PmcA are important for normal growth, morphogenesis and cell wall integrity, but not for viability in Aspergillus nidulans. Microbiology 160:2387–2395. https://doi.org/10.1099/mic.0.080119-0.
39. Powers-Fletcher MV, Jambunathan K, Brewer JL, Krishnan K, Feng X, Galande AK, Askew DS. 2011. Impact of the lectin chaperone calnexin on the stress response, virulence and proteolytic secretome of the fungal pathogen Aspergillus fumigatus. PLoS One 6:e28865. https://doi.org/10.1371/journal.pone.0028865.
40. Elagoz A, Callejo M, Armstrong J, Rokeach LA. 1999. Although calnexin is essential in S. pombe, its highly conserved central domain is dispensable for viability. J Cell Sci 112:4449–4460.
41. Brostrom MA, Brostrom CO. 2003. Calcium dynamics and endoplasmic reticular function in the regulation of protein synthesis: implications for cell growth and adaptability. Cell Calcium 34:345–363. https://doi.org/10.1016/S0143-4160(03)00127-1.
42. Putney JW, Jr, McKay RR. 1999. Capacitative calcium entry channels. Bioessays 21:38–46.
43. Bonilla M, Cunningham KW. 2003. Mitogen-activated protein kinase stimulation of Ca^{2+} signaling is required for survival of endoplasmic reticulum stress in yeast. Mol Biol Cell 14:4296–4305. https://doi.org/10.1091/mbc.E03-02-0113.
44. Rudolph HK, Antebi A, Fink GR, Buckley CM, Dorman TE, LeVitre J, Davidow LS, Mao JI, Moir DT. 1989. The yeast secretory pathway is perturbed by mutations in PMR1, a member of a Ca^{2+} ATPase family. Cell 58:133–145. https://doi.org/10.1016/0092-8674(89)90410-8.
45. Lynes EM, Raturi A, Shenkman M, Ortiz Sandoval C, Yap MC, Wu J, Janowicz A, Myhill N, Benson MD, Campbell RE, Berthiaume LG, Lederkremer GZ, Simmen T. 2013. Palmitoylation is the switch that assigns calnexin to quality control or ER Ca^{2+} signaling. J Cell Sci 126:3893–3903. https://doi.org/10.1242/jcs.125856.
46. Cronin SR, Rao R, Hampton RY. 2002. Cod1p/Spf1p is a P-type ATPase involved in ER function and Ca^{2+} homeostasis. J Cell Biol 157:1017–1028. https://doi.org/10.1083/jcb.200203052.
47. Lustoza AC, Palma LM, Facanha AR, Okorokov LA, Okorokova-Facanha AL. 2011. P(5A)-type ATPase Cta4p is essential for Ca^{2+} transport in the endoplasmic reticulum of Schizosaccharomyces pombe. PLoS One 6:e27843. https://doi.org/10.1371/journal.pone.0027843.
48. Nayak T, Szewczyk E, Oakley CE, Osmani A, Ukil L, Murray SL, Hynes MJ, Osmani SA, Oakley BR. 2006. A versatile and efficient gene-targeting system for Aspergillus nidulans. Genetics 172:1557–1566. https://doi.org/10.1534/genetics.105.052563.
49. Todd RB, Davis MA, Hynes MJ. 2007. Genetic manipulation of Aspergillus nidulans: meiotic progeny for genetic analysis and strain construction. Nat Protoc 2:811–821. https://doi.org/10.1038/nprot.2007.112.
50. Yu JH, Hamari Z, Han KH, Seo JA, Reyes-Dominguez Y, Scazzocchio C. 2004. Double-joint PCR: a PCR-based molecular tool for gene manipulations in filamentous fungi. Fungal Genet Biol 41:973–981. https://doi.org/10.1016/j.fgb.2004.08.001.
51. Soriani FM, Malavazi I, da Silva Ferreira ME, Savoldi M, Von Zeska Kress MR, de Souza Goldman MH, Loss O, Bignell E, Goldman GH. 2008. Functional characterization of the Aspergillus fumigatus CRZ1 homologue, CrzA. Mol Microbiol 67:1274–1291. https://doi.org/10.1111/j.1365-2958.2008.06122.x.
52. Nelson G, Kozlova-Zwinderman O, Collis AJ, Knight MR, Fincham JR, Stanger CP, Renwick A, Hessing JG, Punt PJ, van den Hondel CA, Read ND. 2004. Calcium measurement in living filamentous fungi expressing codon-optimized aequorin. Mol Microbiol 52:1437–1450. https://doi.org/10.1111/j.1365-2958.2004.04066.x.
53. Osmani SA, Pu RT, Morris NR. 1988. Mitotic induction and maintenance by overexpression of a G2-specific gene that encodes a potential protein kinase. Cell 53:237–244. https://doi.org/10.1016/0092-8674(88)90385-6.
54. Song J, Zhai P, Zhang Y, Zhang C, Sang H, Han G, Keller NP, Lu L. 2016. The Aspergillus fumigatus damage resistance protein family coordinately regulates ergosterol biosynthesis and azole susceptibility. mBio 7:e01919-15. https://doi.org/10.1128/mBio.01919-15.
55. Greene V, Cao H, Schanne FA, Bartelt DC. 2002. Oxidative stress-induced calcium signalling in Aspergillus nidulans. Cell Signal 14:437–443. https://doi.org/10.1016/S0898-6568(01)00266-2.